

## Two-Dimensional Quantum Ferromagnets

Carsten Timm<sup>a</sup>, Patrik Henelius<sup>a</sup>, Anders W. Sandvik<sup>b</sup>, S. M. Girvin<sup>a</sup>

<sup>a</sup> Department of Physics, Indiana University, Bloomington, Indiana 47405

<sup>b</sup> Department of Physics, University of Illinois, 1110 West Green Street, Urbana, Illinois 61801

(October 22, 1997)

We present  $1/N$  Schwinger boson and quantum Monte Carlo calculations of the magnetization and NMR relaxation rate for the two-dimensional ferromagnetic Heisenberg model representing a quantum Hall system at filling factor  $\nu = 1$ . Comparing the analytic and numerical calculations, we find that the  $SU(N)$  version of Schwinger boson theory gives accurate results for the magnetization at low temperatures, whereas the  $O(N)$  model works well at higher temperatures.

PACS numbers: 73.40.Hm, 75.40.Mg, 76.50.+g, 75.30.Ds

Two-dimensional quantum magnets have received particular attention in recent years because of advances in materials synthesis associated with high-temperature superconductivity, thin films and surfaces, and semiconductor quantum wells. It has recently come to be appreciated that two-dimensional electron gases in quantum wells subjected to strong magnetic fields in the quantum Hall regime are novel itinerant ferromagnets. The strong external magnetic field quenches the orbital kinetic energy but couples only very weakly to the spin degrees of freedom allowing low energy spin fluctuations to survive.

Two-dimensional ferromagnets exhibit novel topological defects referred to as skyrmions by analogy with the corresponding objects in the Skyrme model in nuclear physics. What is unique about quantum Hall ferromagnets [1,2] is that these defects carry fermion charge and hence their ground state density can be controlled by moving the filling factor away from  $\nu = 1$ . The combination of low energy spin fluctuations and these topological defects dramatically alters the NMR spectrum [3,2] and the specific heat [4].

With the advent of NMR and magnetoabsorption measurements in quantum Hall systems, it is now possible to measure the temperature dependence of the electron magnetization. Recent theoretical work [5] has evaluated the magnetization of this quantum critical system at  $\nu = 1$  using  $SU(N)$  and  $O(N)$  formulations of mean field theory (with  $N = \infty$ ). In this paper we present analytic results for the  $1/N$  corrections to the magnetization and compare them with extensive quantum Monte Carlo simulations. We also present numerical results for the NMR relaxation rate  $1/T_1$ . In addition to their relevance to 2D quantum ferromagnets in general and QHE magnets in particular, these results provide new information on the level of accuracy of large  $N$  expansion methods and show a highly non-trivial difference in the behavior of the  $SU(N)$  and  $O(N)$  models.

Low energy spin fluctuations in quantum Hall ferromagnets at  $\nu = 1$  are expected to be well described by the Heisenberg model [5]. The large  $N$  approach to this model is a systematic expansion around a mean field theory for  $N = \infty$  and has the advantage of being equally

valid at all temperatures  $T$ . Furthermore, even at the mean field level this approach correctly captures the fact that arbitrarily small thermal fluctuations destroy the long range order in two dimensions. An alternative microscopic approach which includes spin-wave corrections to the electronic self-energy has also recently been developed [6]. Trumper *et al.* [7] employ an  $SU(2)$  Schwinger boson theory to describe Gaussian fluctuations in a frustrated 2D antiferromagnet.

We start from the Heisenberg Hamiltonian

$$H = -J \sum_{\langle ij \rangle} \mathbf{S}(i) \cdot \mathbf{S}(j) - B \sum_i S^z(i) \quad (1)$$

on a square lattice, where  $\mathbf{S} \cdot \mathbf{S} = S(S+1)$  at each site. By introducing two Schwinger bosons at each site,  $S^+ = a^\dagger b$ ,  $S^- = b^\dagger a$ , and  $S^z = (a^\dagger a - b^\dagger b)/2$ , subject to the constraint  $a^\dagger a + b^\dagger b = 2S$ , one obtains an equivalent boson Hamiltonian. The  $SU(2)$  spin algebra of this model is generalized to  $SU(N)$  [8]. After going over to the continuum, the  $SU(N)$  Hamiltonian is written in terms of  $N$  bosons  $b_\alpha$  per site,

$$H = \int d^2r \left[ JS(\partial_j b_\alpha^\dagger)(\partial_j b_\alpha) - \frac{J}{N} b_\alpha^\dagger (\partial_j b_\beta^\dagger) b_\beta (\partial_j b_\alpha) - \frac{B}{2a^2} h_\beta^\alpha b_\beta^\dagger b_\alpha \right], \quad (2)$$

where summation over repeated indices is implied and  $a$  is the lattice constant. The bosons are subject to the constraint  $\sum_\alpha b_\alpha^\dagger b_\alpha = NS$ , which picks out the allowed spin states for total spin  $S$ . The matrix  $h_\beta^\alpha = \delta_{\alpha\beta}(-1)^{\alpha+1}$  describes the coupling of the bosons to the magnetic field.

The partition function can be written as a coherent state functional integral over complex fields  $b_\alpha$ . Decoupling the quartic term by means of a Hubbard-Stratonovich transformation one finds

$$Z = \int D^2 b_\alpha D\lambda DQ_j \exp \left( -\frac{1}{\hbar} \int_0^{\hbar\beta} d\tau \int d^2r \mathcal{L}[b; \lambda, \mathbf{Q}] \right)$$

with the Lagrangian density

$$\mathcal{L} = \frac{\hbar}{a^2} b_\alpha^* \partial_0 b_\alpha + JS(\partial_j b_\alpha^*)(\partial_j b_\alpha) + NJQ_j Q_j$$

$$+ iJQ_j b_\alpha^* (\partial_j b_\alpha) - iJQ_j (\partial b_\alpha^*) b_\alpha - \frac{B}{2a^2} h_\beta^\alpha b_\beta^* b_\alpha \\ + \lambda b_\alpha^* b_\alpha - NS\lambda, \quad (3)$$

where  $\lambda$  is an imaginary Lagrange multiplier field which implements the constraint, and  $\mathbf{Q}$  is the real-valued Hubbard-Stratonovich field which acts as a gauge field.

The local equivalence of the groups  $SU(2)$  and  $O(3)$  allows one to also write down an  $O(3)$  boson model equivalent to Eq. (1), which can be generalized to  $O(N)$  [5]. The continuum  $O(N)$  Hamiltonian reads

$$H = \int d^2r \left[ JS (\partial_j b_\alpha^\dagger) (\partial_j b_\alpha) - \frac{3J}{N} b_\alpha^\dagger (\partial_j b_\beta^\dagger) b_\beta (\partial_j b_\alpha) \right. \\ \left. - \frac{B}{a^2} h_\beta^\alpha b_\beta^\dagger b_\alpha \right] \quad (4)$$

with the constraints  $\sum_\alpha b_\alpha^\dagger b_\alpha = NS/3$  and  $\sum_\alpha b_\alpha^\dagger b_\alpha^\dagger = 0$ . The matrix  $h$  contains  $N/3$  copies of the  $O(3)$  generator matrix  $((0, i, 0), (-i, 0, 0), (0, 0, 0))$  along the diagonal. The second constraint means that creating two bosons of kind, say,  $N$  produces a state which is a linear combination of states without two  $N$  bosons added. This constraint restricts the Hilbert space by identifying certain states with one another. In the functional integral it is enforced by a new *complex* Lagrange multiplier  $\mu$ , which enters the Lagrangian as  $\mu^* b_\alpha b_\alpha/2 + \mu b_\alpha^* b_\alpha^*/2$ .

To obtain mean field results, the auxiliary fields  $\lambda$ ,  $\mathbf{Q}$ , and, for  $O(N)$ ,  $\mu$  are set to their values at the saddle point. We denote mean field values by a subscript 0. After Fourier transformation, the boson fields can be integrated out. The values of the auxiliary fields are obtained by solving the saddle-point equations. Because of gauge invariance,  $\mathbf{Q}_0$  can be taken to vanish. For  $O(N)$  we find  $\mu_0 = 0$ . The mean field magnetization  $M_0$  is then found from the free energy and has been given by Read and Sachdev for both models [5].

Another useful quantity is the NMR relaxation rate

$$\frac{1}{T_1} = \frac{A}{\mathcal{N}} \sum_{\mathbf{q}} S(\mathbf{q}, \omega \rightarrow 0), \quad (5)$$

where  $A$  is the hyperfine structure factor, which we assume to be isotropic and momentum independent,  $\mathcal{N}$  is the number of sites, and  $S(\mathbf{q}, \omega)$  is the dynamic structure factor, which is related to the transverse susceptibility by  $S(\mathbf{q}, \omega) = \text{Im } \chi^{+-}(\mathbf{q}, \omega) / (1 - e^{-\beta \hbar \omega})$ . The mean field rate is plotted in Ref. [5], here, we give analytic results for completeness. For  $SU(N)$ ,  $1/T_1 = A n_B (\Lambda_0 + \beta B/2) / (32\pi\beta^2 J^2 S^2)$  and for  $O(N)$ ,  $1/T_1 = A [n_B (\Lambda_0 + \beta B) + n_B (\Lambda_0)] / (16\pi\beta^2 J^2 S^2)$ .

We now turn to  $1/N$  corrections to the magnetization. For the  $SU(N)$  case, fluctuations in the auxiliary fields about their saddle-point values are denoted by  $i\Delta\lambda = \lambda - \lambda_0$  and  $\Delta\mathbf{Q} = \mathbf{Q}$ , respectively. As a short-hand we denote any fluctuation mode by  $r_\ell = \{\Delta\lambda(\mathbf{r}, \tau), \Delta Q_j(\mathbf{r}, \tau)\}$ .

Following the approach outlined in Ref. [9], the partition function is written as a functional integral over the  $r_\ell$ ,

$$Z = \int Dr_\ell e^{-N\mathcal{S}[r_\ell]} \quad (6)$$

with the action  $\mathcal{S} = \mathcal{S}_0 + \mathcal{S}_{\text{dir}} + \mathcal{S}_{\text{loop}}$ , where

$$\mathcal{S}_0 = N^{-1} \text{Tr} \ln G_0^{-1}, \\ \mathcal{S}_{\text{dir}} = \frac{1}{N\hbar} \int_0^{\hbar\beta} d\tau \int d^2r (NJ\mathbf{Q} \cdot \mathbf{Q} - NS\lambda), \\ \mathcal{S}_{\text{loop}} = N^{-1} \text{Tr} \ln (1 + G_0 v_\ell r_\ell).$$

Here, the trace sums over momenta, Matsubara frequencies, and boson flavors  $\alpha$ .  $G_0^\alpha(\mathbf{k}, i\omega_n) \equiv (-i\hbar\omega_n + JSk^2 a^2 - Bh_\alpha^\alpha/2 + a^2\lambda_0)^{-1}$  is the mean field boson Green function, and the  $v_\ell$  are vertex factors describing the coupling of the bosons to the fluctuation  $r_\ell$ . The action can be written as a Taylor series in fluctuations  $r_\ell$ ,  $\mathcal{S} = \sum_{n=0}^{\infty} (n!)^{-1} \mathcal{S}_{\ell_1 \dots \ell_n}^{(n)} r_{\ell_1} \dots r_{\ell_n}$ , where the  $n=1$  term vanishes since we are expanding around a saddle point.  $\mathcal{S}_0$  conspires with the  $r_\ell$  independent part of  $\mathcal{S}_{\text{dir}}$  to form the mean field free energy  $\beta F_0 = N\mathcal{S}^{(0)}$ . The other terms in the series can be found by expanding  $\mathcal{S}_{\text{loop}}$  and  $\mathcal{S}_{\text{dir}}$ . The RPA fluctuation propagator is the inverse of the matrix  $\mathcal{S}^{(2)}$ .

The magnetization is expressed in terms of boson occupation numbers,  $M = 1/N \sum_\alpha h_\alpha^\alpha \langle b_\alpha^\dagger b_\alpha \rangle$ , and the expectation values  $\langle b_\alpha^\dagger b_\alpha \rangle$  are obtained by inserting a constant source term  $\sum_\alpha j_\alpha b_\alpha^\dagger b_\alpha$  into the Hamiltonian in Eq. (2). We apply this procedure to the partition function of Eq. (6) and expand the result in a Taylor series in the  $r_\ell$ . The resulting Gaussian integrals can be evaluated by contractions over  $r_\ell$ . This corresponds to writing down all allowed diagrams with one external  $j_\alpha$  vertex and any number of internal vertices, connecting all internal vertices by RPA propagators. Loops without an external vertex and with one or two internal ones are forbidden since the former vanish in an expansion around a saddle point and the latter are included in the RPA propagator. Fig. 1 shows the diagrams of order  $1/N$ .

Summation over the frequency of the vertical RPA propagator in both diagrams must be done carefully, taking into account normal ordering of operators at equal times. This procedure makes the frequency sums unambiguous and removes a spurious divergence. The details will be given elsewhere [10]. The magnetization can now be calculated numerically. The momentum integrals have a logarithmic UV divergence, which is regularized by a lattice cutoff. The  $1/N$  contributions from both  $\Delta\lambda$  and  $\Delta Q_j$  decrease the magnetization, as intuitively expected.

For the  $O(N)$  model we additionally have to deal with fluctuations  $\Delta\mu$  in the second Lagrange multiplier field, which couple only to  $b_\alpha^\dagger b_\alpha^\dagger$  and  $b_\alpha b_\alpha$ . To order  $1/N$  the only contributions come from the two  $1/N$  diagrams with the vertical propagator replaced by a  $\Delta\mu$  RPA propagator and the direction of the boson Green functions

changed accordingly. The result converges for large momenta and actually increases the magnetization: Mean field theory, which enforces the constraint  $\sum_\alpha b_\alpha^\dagger b_\alpha^\dagger = 0$  only on average, underestimates the magnetization because it contains unphysical contributions from spin multiplets of lower total spin. Analytic results are further discussed below.

In order to test the accuracy of the analytic results, we have carried out Quantum Monte Carlo simulations using the stochastic series expansion method [11], which is ideally suited for the present calculation since it does not introduce any systematic errors. Sufficiently large lattices can be studied so that finite size effects are negligible. The method is based on a Taylor expansion of the density matrix  $e^{-\beta H}$ . Writing  $H$  is terms of its one- and two-body terms,  $H = \sum_{i=1}^M H_i$ , the partition function can be written as [11]

$$Z = \sum_{\alpha} \sum_{n=0}^{\infty} \sum_{S_n} \frac{(-\beta)^n}{n!} \langle \alpha | \prod_{i=1}^n H_{l_i} | \alpha \rangle, \quad (7)$$

where  $S_n$  denotes a sequence of indices  $(l_1, l_2, \dots, l_n)$  with  $l_i \in 1, \dots, M$ , and  $|\alpha\rangle = |S_1^z, S_2^z, \dots, S_N^z\rangle$  is an eigenstate of all the operators  $S_i^z$ . The relative weight in this expression can be made positive definite by adding a suitable constant to  $H$ . For a system of finite  $N$  and  $\beta$  only sequences of finite length contribute significantly and the limit  $n \rightarrow \infty$  poses no problem (the average power  $\langle n \rangle$  is given by  $|E|\beta$ , where  $E$  is the total internal energy).

We want to emphasize an important feature that makes the sampling particularly efficient: The external field is chosen in the  $\hat{x}$  direction. This automatically causes the simulation to become grand-canonical and there are no longer any problems associated with a restricted winding number. If the transverse field is not too weak ( $B/J \gtrsim 0.02$ ), it causes the auto-correlation times of all calculated quantities to become very short, even though only purely local updates are used. Furthermore, it enables easy access to observables involving both diagonal and off-diagonal operators. Details of the implementation will be presented elsewhere [12].

For a  $4 \times 4$  system we have compared our QMC data with exact diagonalization results, and they agree to within statistical errors. Relative errors are typically of the order  $10^{-4}$  for all system sizes considered. For all the field strengths presented in this paper the results for  $16 \times 16$  and  $32 \times 32$  sites agree to this precision (finite-size effects increase with decreasing  $B$ ), and we here present magnetization results for the larger size.

The  $\mathbf{q}$  dependent imaginary time susceptibility is

$$\chi^{+-}(\mathbf{q}, \tau) = \frac{1}{N} \sum_{\mathbf{r}} \langle S^z(\mathbf{r}, \tau) S^z(0, 0) \rangle e^{i\mathbf{q} \cdot \mathbf{r}}.$$

Once it has been calculated, the dynamic structure factor can be obtained by inverting the relation

$$\chi^{+-}(\mathbf{q}, \tau) = \frac{1}{\pi} \int d\omega S(\mathbf{q}, \omega) e^{-\tau\omega}$$

using the maximum-entropy technique [13]. The  $B$  field introduces an additional complication to the analytic continuation since it introduces a delta function peak in the spectral weight at  $\omega = B$  arising from the  $\mathbf{q} = 0$  response. The maximum entropy method cannot resolve separate delta functions in the spectrum and since we are studying relatively small fields this potentially causes problems for the calculation of  $1/T_1$ . We therefore found it useful to separate out the  $\mathbf{q} = 0$  sector before continuing the average  $\sum_{\mathbf{q}} \chi^{+-}(\mathbf{q}, \tau)$ . The results are, however, still sensitive to the somewhat sharp peaks in the spectral function near  $\omega = B$  from momenta near  $q = 0$ ; a problem which becomes worse with increasing system size. We therefore only use  $16 \times 16$  sites for the  $1/T_1$  calculation, which should be sufficient in the interesting temperature regime. We estimate the statistical errors using the bootstrap technique. As with any results obtained by the maximum entropy method, the error estimates have to be viewed with some caution.

Fig. 2 shows the magnetization for spin  $S = 1/2$  and magnetic field  $B = 0.1 J$ . The results are typical for all fields considered ( $0.02 \leq B/J \leq 0.32$ ). The  $SU(N)$  results agree with Monte Carlo data only at the lowest temperatures. In fact, at low temperatures the  $SU(N)$  mean field magnetization is known to agree with the non-interacting magnon approximation for the Heisenberg model up to exponentially small corrections. This is not the case for the  $O(N)$  model. There is a distinct crossover to moderate and high temperatures, where the  $O(N) 1/N$  results agree quite well with the data, whereas the  $SU(N) 1/N$  correction eventually becomes much too large. The main differences between the systems studied above are that (i) the analytic calculations use a continuum approximation, and (ii) the leading terms in the  $1/N$  expansion do not include skyrmion effects, whereas the Monte Carlo simulations in principle do. Both effects should lead to discrepancies at temperatures of order  $J$  and higher. We will further pursue the question of why the  $O(N)$  model works better than the  $SU(N)$  model at most temperatures in a subsequent paper [10].

Experimental data by Barrett *et al.* [3] show a more rapid drop off at higher temperatures, probably due to disorder affecting the normalization of the data. In Fig. 3 we compare our results with recent magnetoabsorption measurements by Manfra *et al.* [14]. The experiments agree well with our  $O(N) 1/N$  and Monte Carlo results except at low temperatures. The calculations have been done for  $B = 0.32 J$ , which is the experimental field corrected for finite width of the quantum well [14]. The approximation used by Kasner and MacDonald [6] leads to a much higher magnetization than obtained here.

In summary, we find from our comparison of Monte Carlo and analytic approaches that the  $SU(N)$  model cor-

rectly captures the low-temperature magnetization and that the first  $1/N$  correction to the  $O(N)$  model gives accurate results at higher temperatures. We also find that the NMR relaxation rate evaluated by analytic continuation from the Monte Carlo data agrees rather well with the mean field result, as shown in Fig. 4. Both the  $1/N$  and Monte Carlo calculations were rather involved. Technical details will be presented elsewhere [10,12].

We thank S. Sachdev and A. MacDonald for helpful discussions. The work at Indiana is supported by NSF DMR-9714055 and NSF CDA-9601632, and at Illinois by NSF DMR-9520776. C.T. acknowledges support by the Deutsche Forschungsgemeinschaft. P.H. acknowledges support by the Ella och Georg Ehrnrooths stiftelse.

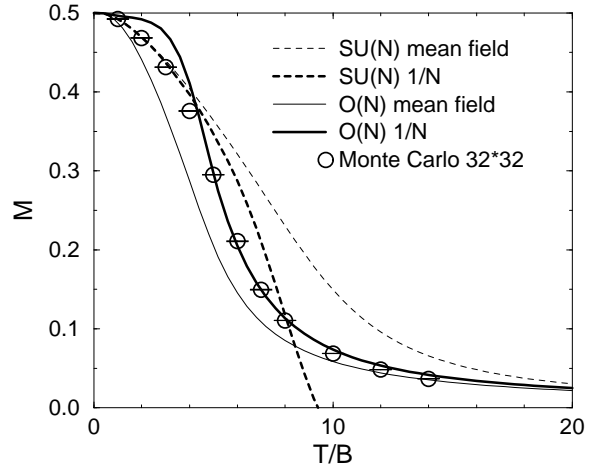


FIG. 2. Magnetization of a 2D quantum ferromagnet with magnetic field  $B = 0.1 J$  and spin  $S = 1/2$ .

- [1] S.L. Sondhi, A. Karlhede, S.A. Kivelson, and E.H. Rezayi, Phys. Rev. B **47**, 16419 (1993).
- [2] R. Côté, A.H. MacDonald, Luis Brey, H.A. Fertig, S.M. Girvin, H.T.C. Stoof, Phys. Rev. Lett. **78**, 4825 (1997).
- [3] S.E. Barrett *et al.*, Phys. Rev. Lett. **72**, 1368 (1994); *ibid.* **74**, 5112 (1995).
- [4] V. Bayot *et al.*, Phys. Rev. Lett. **76**, 4584 (1996); *ibid.* **79**, 1718 (1997).
- [5] N. Read and S. Sachdev, Phys. Rev. Lett. **75**, 3509 (1995).
- [6] M. Kasner and A.H. MacDonald, Phys. Rev. Lett. **76**, 3204 (1996).
- [7] A.E. Trumper, L.O. Manuel, C.J. Gazza, and H.A. Cecatto, Phys. Rev. Lett. **78**, 2216 (1997).
- [8] D.P. Arovas and A. Auerbach, Phys. Rev. B **38**, 316 (1988).
- [9] A. Auerbach, *Interacting Electrons and Quantum Magnetism* (Springer, New York, 1994).
- [10] C. Timm *et al.* (unpublished).
- [11] A. W. Sandvik and J. Kurkijärvi, Phys. Rev. B **43**, 5950 (1991); A.W. Sandvik, J. Phys. A **25**, 3667 (1992).
- [12] P. Henelius *et al.* (unpublished).
- [13] J.E. Gubernatis *et al.*, Phys. Rev. B **44**, 6011 (1991).
- [14] M.J. Manfra *et al.*, Phys. Rev. B **54**, R17327 (1996).

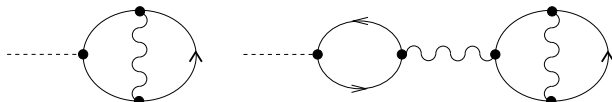


FIG. 1. Diagrams of order  $1/N$  for  $\langle b_\alpha^\dagger b_\alpha \rangle$ . Solid lines denote boson mean field Green functions, wiggly lines are RPA fluctuation propagators, and dashed lines are external  $j_\alpha$  insertions.

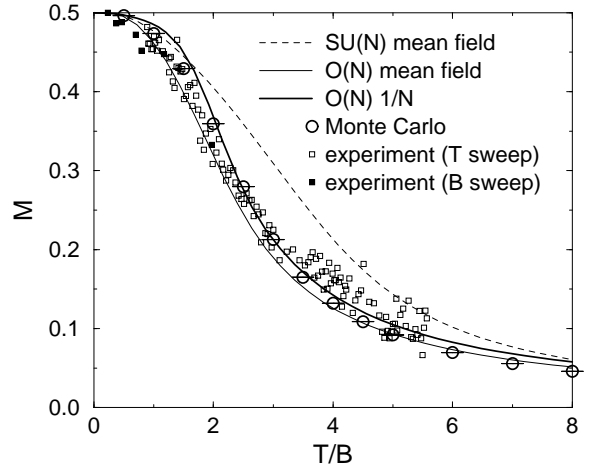


FIG. 3. Magnetization for  $B = 0.32 J$  compared with experiments from Ref. [14].

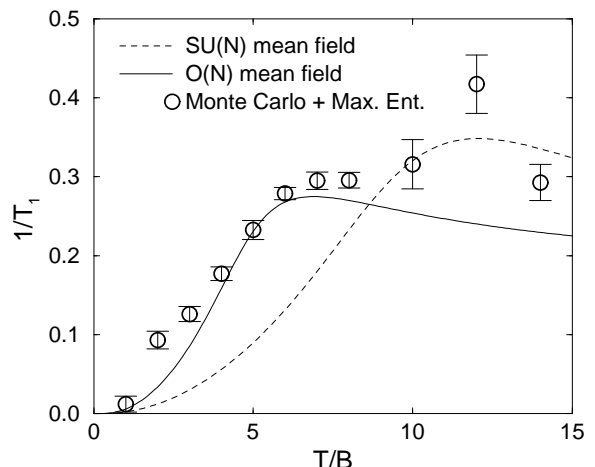


FIG. 4. NMR relaxation rate  $1/T_1$  for  $B/J = 0.1$ .